

## Evaluating the mechanical performance of Very Thin Asphalt Overlay (VTAO) as a sustainable rehabilitation strategy in urban pavements

M. Sol-Sánchez✉, G. García-Travé, P. Ayar, F. Moreno-Navarro, M.C. Rubio-Gámez

Laboratory of Construction Engineering (LabIC.UGR), Department of Construction Engineering (ICPI), School of Civil Engineering (ETSICCP), University of Granada, (Granada, Spain)  
✉msol@ugr.es

Received 15 April 2016  
Accepted 29 November 2016  
Available on line 26 July 2017

**ABSTRACT:** Very Thin Asphalt Overlay (VTAO) has been introduced as an alternative to traditional thick overlays, seal coats, and micro-surfacings. Nonetheless, there are some challenges that still remain regarding the application of VTAOs (such as mixture type, cohesiveness, wear resistance, cracking and durability), particularly in heavy traffic urban areas. Therefore, this paper presents an extensive comparative evaluation of the mechanical performance, durability and safety issues (cohesiveness, adhesiveness, ageing, cracking, plastic deformation, permeability, macrotexture, skid and wear resistance, and fuel resistance) of a VTAO (20 mm thick) and a high performance BBTM 11B (35 mm thick), commonly used as an open-graded mixture for pavement overlays. The results demonstrated that VTAO is an appropriate material for urban pavements as it provides good durability and resistance to the propagation of defects. Nonetheless, further studies are required to improve its behavior under distresses related to plastic deformations and safety properties.

**KEYWORDS:** Adherence; Durability; Fatigue; Permeability; Mechanical properties

**Citation/Citar como:** Sol-Sánchez, M.; García-Travé, G.; Ayar, P.; Moreno-Navarro, F.; Rubio-Gámez, M.C. (2017) Evaluating the mechanical performance of Very Thin Asphalt Overlay (VTAO) as a sustainable rehabilitation strategy in urban pavements. *Mater. Construcc.* 67 [327], e132 <http://dx.doi.org/10.3989/mc.2017.05016>

**RESUMEN:** *Evaluación del comportamiento mecánico de capas bituminosas ultra delgadas como una adecuada estrategia para la rehabilitación de pavimentos urbanos.* Las capas bituminosas ultra delgadas para rehabilitación superficial de carreteras son una alternativa a las tradicionales capas asfálticas, riegos bituminosos y micro-aglomerados. No obstante, aún son numerosos los aspectos a estudiar para la generalización de su uso, particularmente en zonas urbanas con elevado tráfico. Así, este artículo recoge un análisis comparativo del comportamiento mecánico, durabilidad y factores de seguridad (evaluando parámetros como cohesividad, adhesividad, envejecimiento, fisuración, deformaciones, permeabilidad, macrotextura, y resistencia al deslizamiento, al desgaste y a los combustibles) entre una capa delgada de 20 mm de espesor, y una mezcla discontinua de altas prestaciones (BBTM-11B con 35 mm), comúnmente utilizada en capas de rodadura. Los resultados indican que puede ser una adecuada solución para pavimentos urbanos dada su durabilidad y resistencia a la propagación de fallos. No obstante, se requieren futuros estudios centrados en la mejora de parámetros de seguridad y de su resistencia a las deformaciones permanentes.

**PALABRAS CLAVE:** Adherencia; Durabilidad; Fatiga; Permeabilidad; Propiedades mecánicas

**ORCID ID:** M. Sol-Sánchez (<http://orcid.org/0000-0003-3756-7556>); G. García-Travé (<http://orcid.org/0000-0002-5101-1610>); P. Ayar (<http://orcid.org/0000-0002-9856-5995>); F. Moreno-Navarro (<http://orcid.org/0000-0001-6758-8695>); M.C. Rubio-Gámez (<http://orcid.org/0000-0002-1874-5129>)

**Copyright:** © 2017 CSIC. This is an open-access article distributed under the terms of the Creative Commons Attribution License (CC BY) Spain 3.0.

## 1. INTRODUCTION

Transportation infrastructures play a fundamental role in the economic growth of nations. Over the last three decades, the volume of traffic in highway networks has notably increased (1). Nonetheless, in the field of construction engineering, sustainability issues have been of increasing concern (2). Therefore, the optimization of the maintenance activity of highway and road networks can be considered as a critical aspect to be solved. Clearly, the main aim of rehabilitation and maintenance programs is to extend the service life of these infrastructures. Thus, highway agencies worldwide are attempting to find the most cost-effective and efficient solutions to achieve this goal (3). Traditionally, dense-graded mixture overlays (with a thickness around 50 mm) have been used as a rehabilitation action for asphalt pavements. Later, in order to diminish the consumption of natural resources and due to the development of modified bitumen, other types of gap-graded mixtures with a reduced thickness (around 30-40 mm) such as BBTM or SMA, have successfully substituted the traditional dense-graded mixtures. In recent years, whilst there are other alternative rehabilitation methods (seals, micro-surfacings, etc.), budget limitations and environmental considerations have encouraged highway agencies to use Very Thin Asphalt Overlay (VTAO) as a new rehabilitation strategy (4-6). According to available scientific references, there is no maximum determined thickness for VTAOs, but based on previous studies it appears that a thin overlay refers to an overlay with a maximum thickness of 38 mm (4-7). Additionally, World Road Association (PIARC) has defined thin asphalt surfacing and very thin asphalt surfacing as layers which have an average laying thickness of 30 to 50 mm and 20 to 25 mm respectively (5). Usually, VTAO can be efficiently utilized as a rehabilitation method for pavements with an adequate structure and in which initial symptoms of distress (e.g. block cracking, longitudinal cracking in the wheel path, shallow rutting, raveling, oxidation, and loss of skid resistance) have appeared (8).

As reported by some researchers, VTAOs provide certain environmental benefits such as reducing rolling noise level (4, 5) or diminishing the rolling resistance, which might decrease CO<sub>2</sub> emissions (5). Furthermore, some investigations have revealed the strong anti-spray properties, efficient light reflection, and good skid resistance of VTAOs (4, 5). The cost-effectiveness of VTAOs has also been reported in some studies, particularly in the US (4, 6). For instance, according to Chen and Scullion (4), the total costs for utilizing a 25 mm VTAO are 30% less than a traditional 50 mm overlay. In this regard, the fast paving operation of VTAOs results in shorter periods of closure to traffic flow (5). Consequently, VTAOs are introduced as an alternative to seal

coats or micro-surfacings (4) and they can be used primarily for improving ride quality, maintaining surface geometrics (i.e. preserving the road grade and slope), decreasing noise generation, reducing life cycle costs, and providing a longer-lasting service (7, 9).

Both the mechanical performance and durability of VTAOs directly depend on the mixture used, environmental conditions, and traffic loading. Clearly, the bearing capacity of lower layers and distress levels of the existing pavement must be investigated before paving a VTAO as a rehabilitation method (5). Based on the results of some studies, the mechanical performance of VTAOs in terms of crack resistance was shown to be satisfactory (4, 6). However there are still some issues that require investigation, given the limited information regarding the long and short-term performance of VTAOs. In the US, there have been some efforts to develop comprehensive instructions for the design and construction of VTAOs, as shown, for instance, by the Texas Department of Transportation (TxDOT) in their introduction of a set of specific requirements for the application of VTAOs (4). Utilizing proper mixtures for VTAOs based on environmental and traffic conditions is a matter of critical importance (5, 6). Usually, dense-graded, open-graded and gap-graded (known in Europe as PA and BBTM), and Stone Matrix Asphalt (SMA) have been used for paving VTAOs based on rehabilitation requirements (4, 5). Further, SMA has already been shown to be a suitable mixture for paving a VTAO (6). Additionally, for improving workability —which is a problem owing to the high cooling rate during the paving processes of VTAOs — warm mixes can be used (6). Furthermore, it is recommended that rubber or polymer modified binders can be employed for laying VTAOs, notably in heavy traffic roads to improve mechanical behavior, durability, and skid resistance (5, 7). Regarding this issue, it was found that VTAO constructed with a polymer modified binder has a superior performance in terms of resistance to fatigue and reflective cracking in comparison with VTAO constructed with a rubber modified binder when a traditional hot mix is used (10). However, a number of challenges have been identified in relation to using VTAOs such as the bonding between the VTAO and the lower layer (interlayer cohesiveness), wear resistance (particularly to studded tires), susceptibility to cracking (structural defects in the lower layers), skid resistance, and durability under heavy traffic loads (4, 5, 8). Because of this fact, and due to the high traffic stresses in roads and highways, the application of VTAOs in these types of pavements is limited, while their use in urban pavements has a higher potential. Nonetheless, urban pavements also support high efforts under certain circumstances (high exposure to environmental agents, high shear efforts due to

reduced radius of gyration and braking zones, slow traffic, etc.), and further research is necessary in order to offer stronger assurances regarding the use of VTAO as a rehabilitation solution for these types of pavements.

Based on the issues just described, this article aimed to evaluate the mechanical performance of VTAOs as a rehabilitation strategy for urban pavements. For this purpose, a VTAO with thickness of 20 mm was studied using a range of tests (internal cohesion, resistance to climate deterioration, resistance to plastic deformations and fatigue cracking, skid resistance, fuel resistance and permeability), and the results were compared with those produced by a high performance BBTM 11B.

## 2. EXPERIMENTAL DESIGN

### 2.1. Materials

For this study, two types of asphalt mixtures were used: a VTAO mixture (referred as VTAOM in this paper) and a BBTM 11B (employed as a control

commonly used as overlay in asphalt pavements. The gradations of studied mixtures are depicted in Figure 1.

As can be observed, the maximum size of aggregates in the VTAO mixture (referred to as VTAOM in this paper) is 8 mm (in order to apply this mixture in layers of reduced thickness). Ophitic and limestone aggregates were used as coarse and fine fractions respectively (sand and filler) for preparing VTAOM. Ophitic aggregates were used to meet the demands for high polish and wear resistance in such a thin asphaltic layer while limestone aggregates were used to improve the durability by virtue of a better affinity with the bitumen (11). Further, a SBS (styrene-butadiene-styrene) polymer-modified bitumen (BM3b) was used to manufacture the VTAOM. The optimum bitumen content of the VTAOM was fixed at 5.3% by the total weight of mixture (Table 1), defined from the results obtained in the mix design procedure.

For the BBTM 11B (EN 13108-2) (12), its gradation (with a maximum size of 11 mm) was also formed using ophitic and limestone aggregates for

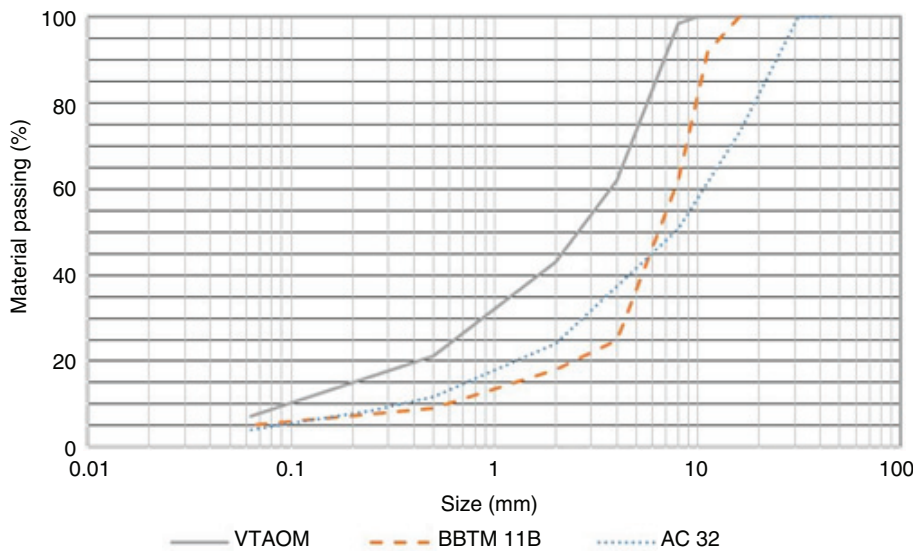


FIGURE 1. The aggregate gradation curves for studied mixtures.

TABLE 1. Properties of the mixtures studied and their optimum bitumen content.

Property (unit)	Standard	VTAOM	BBTM 11B	AC 32
Optimum bitumen content (%)	-	5.3	5.0	3.8
Bulk density (g/cm <sup>3</sup> )	UNE-EN 12697-6	2.652	2.498	2.423
Air void (%)	UNE-EN 12697-8	4.100	12.100	5.800
Voids in Mineral Aggregate (%)	UNE-EN 12697-8	17.500	24.200	14.600
Marshall stability (kN)	UNE-EN 12697-34	19.900	-	16.600
Marshall flow (mm)	UNE-EN 12697-34	3.750	-	2.4100
Particle loss (%)	UNE-EN 12697-17	-	3.000	-

the coarse and fine fractions, respectively. Cement was used as filler in this mixture. The binder used for manufacturing BBTM 11B was a polymer (SBS) modified bitumen type BM3c. According to Table 1, the optimum bitumen content for BBTM 11B is equivalent to 5.0% of the total weight of mixture.

In order to evaluate the mechanical performance of VTAOM and BBTM 11B as thin overlays, an AC 32 mixture (EN 13108-1) (13) containing limestone aggregates (i.e. coarse, fine, and filler fractions) was used as the base asphaltic layer in some of the tests developed in this study. The gradation used in AC 32 is displayed in Figure 1. A 35/50 penetration grade bitumen was used for producing this mixture. As shown in Table 1, the optimum bitumen content for AC 32 was specified at 3.8% of the total weight of the mixture. The surface appearance of the three mixtures used in this study after their compaction can be observed in Figure 2.

To develop an adequate adhesiveness between the thin overlays (VTAOM and BBTM 11B) with the base asphaltic layer (AC 32), an ECR SBS modified bitumen emulsion (C60BP4) was selected as

tack coat. A 2.0 kg/m<sup>2</sup> dosage of this emulsion was selected to provide an adhesive interlayer between the VTAOM and AC 32 (since the maximum aggregate size of VTAOM is considerably low, it is necessary to provide a tack coat with a considerably high dosage of emulsion in order to avoid the appearance of distresses related to a lack of adhesion such as slippage, striping, etc.). The quantity of emulsion sprayed between BBTM 11B and AC 32 was equal to 0.6 kg/m<sup>2</sup>, which is the common dosage used for these types of interlayers (5).

## 2.2. Main laboratory tests

The analysis of the mechanical behavior of the VTAOM and BBTM 11B was based on the main issues of concern regarding its application in urban pavements (cohesiveness, adhesiveness, thermal susceptibility, ageing, cracking, plastic deformation, permeability, macrotexture, skid and wear resistance, and fuel resistance). Table 2 lists the testing plan developed for each type of overlay asphalt mixture.

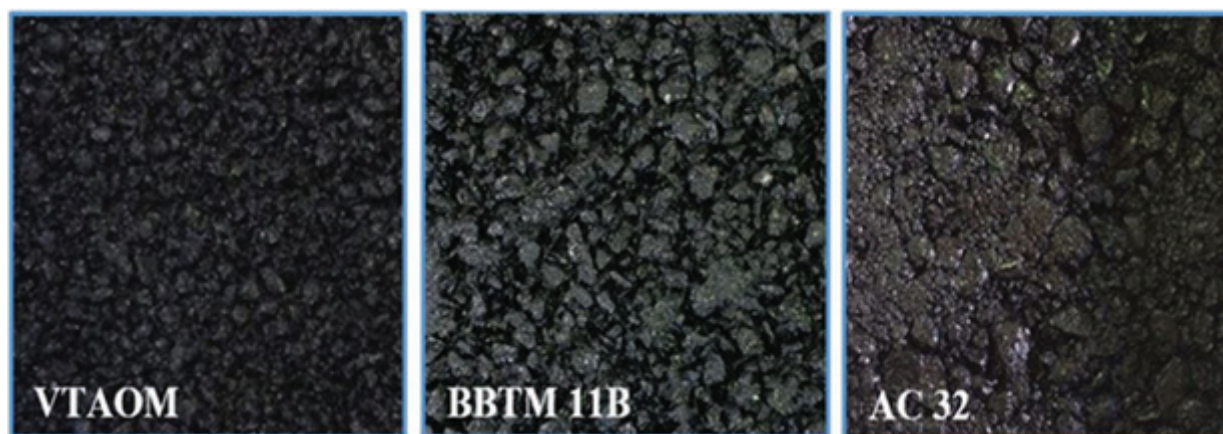


FIGURE 2. The surface appearance of the compacted mixtures.

TABLE 2. Testing plan carried out for each overlay asphalt mixture studied.

Properties	Test	Specimen	Temperature (°C)	Observations
Internal cohesiveness	UCL	3	25	-
Moisture susceptibility	UCL	3	25	-
Thermal susceptibility	UCL	9	0, 30 and 60	-
Ageing	UCL	9	25	Different ageing durations (2, 6 and 12 h)
Plastic deformations	Cyclic triaxial	3	40	10000 cycles
Fatigue cracking and interlayer adhesiveness	UGR-FACT	18	10, 20 and 30	Stress levels: 335 and 500 kPa Specimens: base+surface layer
Permeability	LCS permeameter	2	Ambient	Specimens: base+surface layer
Surface macrotexture	Sand patch	2	Ambient	Specimens: base+surface layer
Skid and wear resistance	Accelerated polishing	4	Ambient	Specimens: base+surface layer
Fuel resistance	Immersing in diesel	3	25	-

### 2.2.1. Cohesiveness, adhesiveness, thermal susceptibility, and ageing tests

A similar procedure to that used in the UCL method (14) was employed to evaluate the behavior of the mixtures (VTAO and BBTM 11B) in terms of cohesiveness, adhesiveness, thermal susceptibility and ageing resistance. This method is based on the particle loss test (EN 12697-17) (15), where Marshall specimens (manufactured using 50 blows per side) are located in a Los Angeles machine (under 200 rotational cycles) (Figure 3A). To evaluate the cohesiveness of the mixtures, the weight loss is measured at 25°C (16). Mixture adhesiveness can be analyzed by measuring the increase of the weight losses of the mixture when the specimens are immersed in water at 60 °C for 24 hours. Moreover, thermal susceptibility can be evaluated by studying the variations in the weight losses when the test is carried out at various temperatures (10 and -10 °C). Finally, the study of the ageing resistance of the mixtures was conducted by exposing

the specimens (placed in a special metallic device) to different ageing conditions (the specimens were kept in a convection oven at 163 °C for 2, 4, and 8 hours before being tested).

### 2.2.2. Resistance to plastic deformations

To analyze the resistance to plastic deformations of the VTAO and BBTM mixtures, The cyclic triaxial confined test based on UNE-EN 12697-25 (part B) standard (17) was conducted on cylindrical specimens with a diameter of 101.6 mm and height of 63 mm (Figure 3B). These specimens (compacted by applying 50 blows per side with a Marshall standard hammer) were tested using a 120 kPa constant confinement stress (in order to simulate the generated stress due to the presence of an existing mass around the loading zone), and a 300 kPa cyclic axial load with a frequency of 3 Hz (which simulates the stresses generated by traffic). The triaxial tests were carried out at 40 °C, applying 10,000 load cycles.



FIGURE 3. Visual appearance of the configuration of the tests developed in this study.

### 2.2.3. Cracking resistance and interlayers adhesiveness

The UGR-FACT (University of Granada – Fatigue Asphalt Cracking Test) method was used to examine the combined action of the traffic loads and thermal gradients on the fatigue cracking resistance and interlayer adhesiveness of the mixtures studied (18-20). This test method simulates the efforts that lead to the failure of an asphalt pavement (Figure 3C). The test device consists of a base (Figure 4a), two supports where the specimen is fixed (Figure 4b), and a load application plate (Figure 4c). The base has a platform that is composed of two sloping surfaces with two rails that allow for the sliding of the supports, and two vertical spindles that are used to measure vertical deformations in the upper part of the test specimen (Figure 4d). The two supports are composed of a carriage that is adapted to the shape of the rail at the base (leading to effective load transmission), and a support plate (to which the test specimen is attached with epoxy resin) where the horizontal deformation gauges (LVDT) are located (Figure 4e). Furthermore, under these support plates, two elastic elements are placed in order to allow for the flexion of the specimen (Figure 4f) and a spring that simulates the foundation layers (Figure 4g). The distance between the supports can vary according to the type of deterioration that needs to be reproduced (e.g. a crack, pre-crack, dilatation joint, pothole, etc.). Finally, the load application plate is composed of a piece of steel that is thick enough to prevent deformations during the load application (thus avoiding differential errors due to its own deformation) whilst providing a flat surface for the vertical deformation gauges (Figure 4e).

Thus, the UGR-FACT method is capable of evaluating both the mechanical performance and

interlayer adhesiveness of asphalt layers, using various specimens that simulate pavement structures. For this purpose, specimens (with a dimension of  $300 \times 300 \times 90$  mm) composed of a 70 mm AC 32 mixture base layer and a 20 mm VTAOM surface layer (bonded with  $2 \text{ kg/m}^2$  of emulsion) were manufactured using a vibratory compactor. Following the manufacture of these samples, they were sawed into smaller prismatic specimens (with dimensions of  $220 \times 60 \times 90$  mm) that were used for testing with the UGR-FACT method. Other specimens composed of a 70 mm AC32 base layer and a 35 mm BBTM 11B surface layer were manufactured using a similar procedure, but with a dosage of emulsion equal to  $0.6 \text{ kg/m}^2$  to ensure the adherence between layers. Finally, the  $300 \times 300 \times 105$  mm compacted specimens were sawed into smaller specimens of  $220 \times 60 \times 105$  mm for testing with the UGR-FACT method.

The fatigue cracking resistance of these specimens was evaluated using the UGR-FACT test at three different temperatures of 10, 20 and 30 °C. In addition, to assess the influence of traffic loading, these tests were carried out at two different levels of traffic — 335 and 500 kPa — to simulate medium and high stress levels respectively. Similarly, a frequency of 5 Hz was used to simulate heavy traffic conditions at 80-100 km/h. In order to obtain a representative profile of the mechanical response of the studied asphaltic layers, for each type of mixture, temperature, and load conditions used, three specimens were tested.

To evaluate the cracking resistance and interlayer adhesiveness, different phases of degradation in the specimens are considered during the UGR-FACT tests. These phases are displayed in Figure 5, where the first phase is related to the occurrence of plastic deformations and other visco-elastic phenomena (21). The modulus of the base layer and its

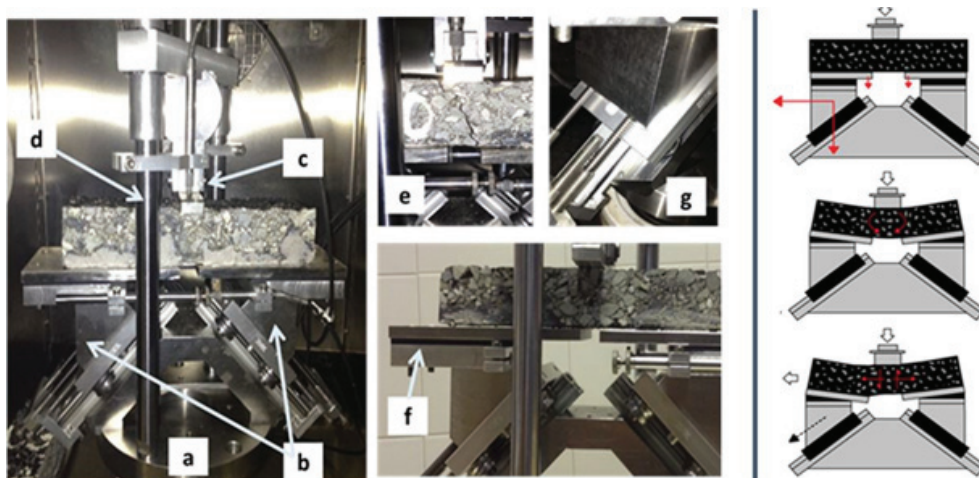


FIGURE 4. UGR-FACT test device.

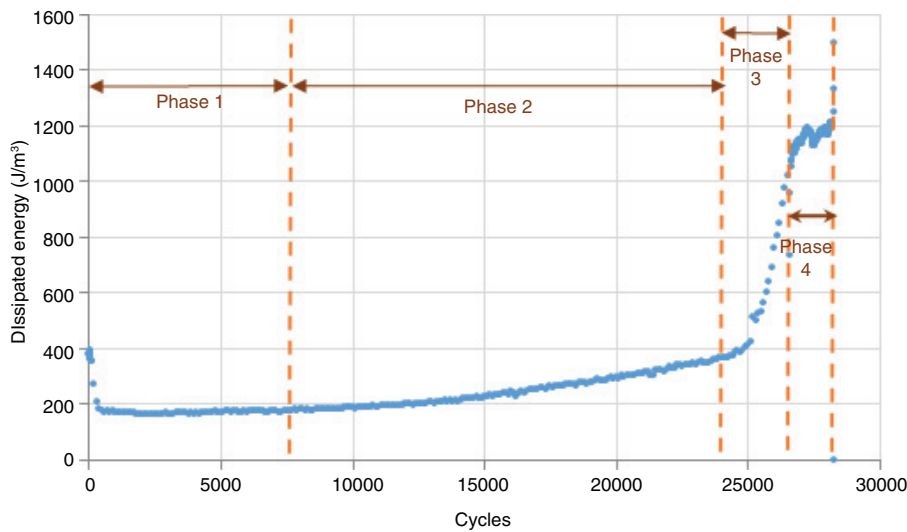


FIGURE 5. Steps during fatigue cracking test of multilayer specimens.

horizontal deflection were determined at the bottom, which allows for identifying the provided bearing capacity by surface course. The second phase (the longest) is related to the development of crack damage and deterioration of the base layer (AC 32). In this phase, the number of cycles required to induce the appearance of macro-cracks in the base layer were determined (which is partly determined by the protective capacity of the surface layer used). The third phase shows the propagation speed of defects (macro-cracks) from the base layer to the surface, and the fourth phase illustrates the number of cycles for which the surface layer is able to overcome damage generated by the lower layers. Hence the ability of the used surface layer to prevent the propagation of the defects (measured as number of cycles) is a fundamental result in this test. It is worth mentioning that such an increase in the amount of dissipated energy during the test (y axis) corresponds with the increasing damage in the material.

The results are expressed in terms of dissipated energy, and the damage produced in the specimen is quantified in accordance with the fact that only the difference in dissipated energy from one cycle to another causes degradation in the material (21). Thus, the cumulative RDEC (Ratio of Dissipated Energy Change, Equation [1]) is used to analyze the development of the damage produced in the specimen, and the Mean Damage Parameter ( $\gamma$ ) [2] is a value used to establish a reference for the resistance to fatigue cracking of the pavement (22).

$$RDEC_{n+1} = \frac{\omega_{n+1} - \omega_n}{\omega_n} \quad [1]$$

Where  $\omega_n$  is the energy dissipation produced in loading cycle  $n$  (in  $J/m^3$ ); and  $\omega_{n+1}$  is the energy dissipation in loading cycle  $n+1$  (in  $J/m^3$ ).

$$\gamma = \frac{\sum_{i=1}^{N_f} RDEC_i}{N_f} \quad [2]$$

Where  $N_f$  is the failure cycle of the specimen.

#### 2.2.4. Permeability

This test is used to measure the drainage capacity of pavement wearing courses. This property is directly related to the void content, which is determined by the type of mineral skeleton, bitumen content and compaction level of the asphalt layer. For determining this parameter, the LCS permeameter (Figure 3D) was used according to NLT-327/00 standard (23), which requires the manufacture of three specimens of each type of pavement studied. Each specimen has a section of  $300 \times 300$  mm, and a height corresponding to the thickness of the road pavement (therefore the specimens were similar to those prepared for the UGR-FACT method described in the previous section). To conduct this test, the LCS permeameter was placed on on each sample. The transparent cylinder should be filled with water 15 cm above the upper measuring mark. The cylinder was then emptied on the surface of the specimen and the time taken to discharge the cylinder between upper and the bottom marks was measured (24). Finally, based on an abacus that was presented in NLT-327/00 standard (23), the permeability coefficient (cm/s) of the pavement can be specified.

#### 2.2.5. Surface macrotexture

The surface texture of asphalt pavements can directly affect their skid resistance (25). The purpose of this test is to determine the average depth of

the surface macrotecture by a volumetric technique, which is also known as the sand patch test, based on NLT-335/00 standard (26). To carry out this test, three test specimens were used with the same dimensions described in the last two sections (horizontal surface of  $300 \times 300$  mm, and a height that will vary as a function of the type of mixture used in the surface layer, 90 mm for the AC32+VTAOM, and 105 for the AC32+BBTM 11B). This test is conducted by spreading a known volume of silica sand ( $25,000 \text{ mm}^3$ ) onto the surface of the samples, over a circular area that is clean and dry. A wooden disc with a hard rubber surface was used to spread the silica sand until a circular area with a radius of between 5 and 18 cm was achieved (Figure 3E). Once the circle appeared, its diameter was measured with calipers, and the average depth of macrotecture (H) was calculated according to Equation [3]. This test procedure was conducted four to five times on a single specimen, creating a circle on the central part of the specimen, and a circle in each of its corners.

$$H = \frac{4V}{\pi \cdot D^2} \quad [3]$$

where V is the volume of the granular material ( $\text{mm}^3$ ), and D is the diameter of the circle area (mm).

#### 2.2.6. Skid and wear resistance

This test is conducted to determine the skid and wear resistance of surface courses, and it is an adaptation of the test described in EN 1097-8 standard (determination of accelerated polishing coefficient) (27). Accordingly, eight specimens were manufactured with the mixtures on the top (four with the VTAOM and the other four with the BBTM 11B) and a resin on the bottom. The friction coefficient of each specimen was determined using a standard pendulum (obtained as an average value from five drops of the pendulum on each specimen) (Figure 3F). After obtaining the initial friction coefficient, the specimens were placed on the accelerated polishing machine to wear down the surface and simulate pavement degradation, according to the UNE-EN 1097-8 procedure. After this polishing process, the pendulum test was repeated in each specimen to determine variations in the friction coefficient. Prior to conducting the pendulum test, it is important to ensure that the samples are clean by submerging them in water for 20 min in order to remove any traces of emery.

#### 2.2.7. Resistance to fuels

The purpose of this test is to determine the resistance of bituminous mixtures against fuel attacks and it is conducted according to EN 12697-43 standard (28). The procedure involves preparing three

cylindrical specimens using a Marshall compactor (50 blows per side) for each type of mixture studied. After determining the density of each specimen, they are immersed in diesel for a period of 24 hrs. Each specimen is then washed with water until the released water from the washed specimen has a constant pH of  $\pm 0.5$ . The test samples were then carefully cleaned and placed in a chamber at  $25^\circ\text{C}$  for 24 hrs. Following this, the loss of mass was determined by weighing the sample. If the loss is greater than 5%, the test is finished. In contrast, when the loss is equal to or less than the specified value, the specimens are brushed with a steel brush that makes epicyclic movements for 120s according to EN 12697-43. For each group of samples the A, B and C parameters were calculated where A is the loss of mass after immersion in fuel (%), B is the loss of mass after the brushing test (%) and C indicates the total mass lost (%) after chemical and abrasive action (Figure 3G). The category of fuel resistance in this test was assigned according to EN 12697-43 as follows:

- If  $B \leq 5\%$  and  $B < 1\%$ , the mixture has a good resistance to fuel.
- If  $A \leq 5\%$  and  $1\% \leq B \leq 5\%$ , the mixture has a moderate resistance to the fuel.
- If  $A > 5\%$  or  $B > 5\%$ , the mixture has a low resistance to that fuel.

### 3. RESULTS AND DISCUSSION

#### 3.1. Cohesiveness, adhesiveness, thermal susceptibility, and ageing tests

Figure 6 shows the internal cohesion and adhesion (moisture susceptibility) of BBTM 11B and VTAOM as a function of mass lost following specific climate conditioning designed to evaluate these properties. As can be observed, the VTAOM recorded a lower percentage loss of mass after both dry and water conditioning, which indicates that this mixture presents better internal cohesion whilst offering lower susceptibility to moisture compared with the BBTM 11B. These findings suggest that the VTAOM could offer higher resistance to the detachment of aggregates (stripping), particularly under moist conditions, which is considered to be one of the main sources of distress in urban asphalt pavements (29).

Figure 7 shows the variation in mass loss depending on the test temperature, which represents the thermal susceptibility of the studied mixtures. According to this figure, the eventual aggregate loss for these mixtures is more likely to occur at lower temperatures (winter) due to the more brittle behavior of the bitumen (30) that leads to the loss of adhesiveness. Nonetheless, it can be noted that the VTAOM showed lower values of aggregate loss when the temperature decreased, thus indicating

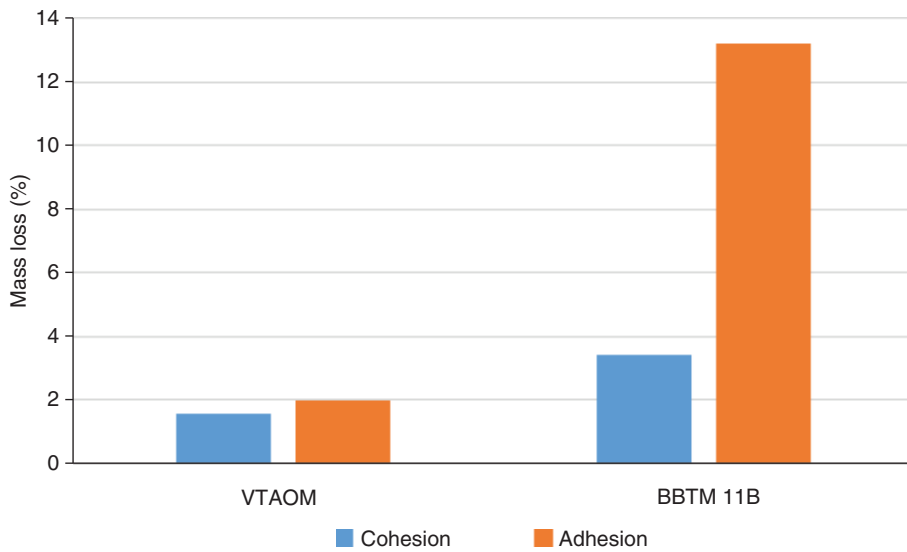


FIGURE 6. Internal cohesion and adhesion of VTAOM and BBTM 11B.

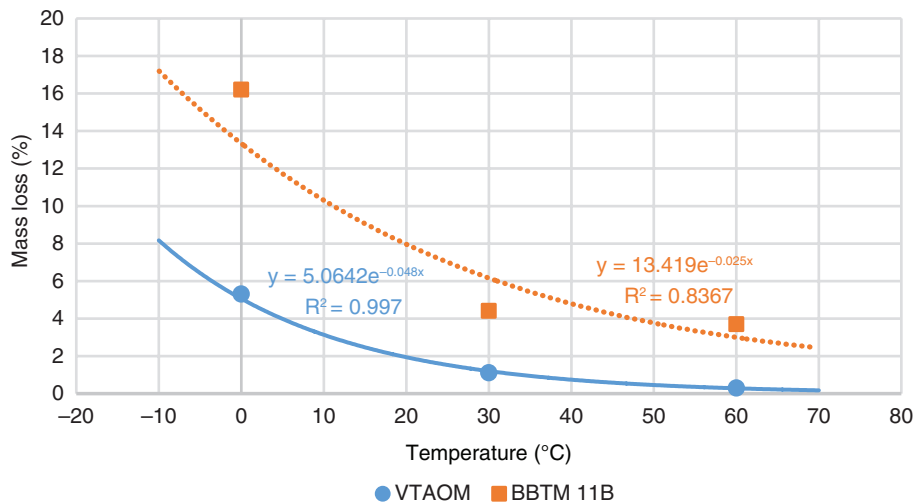


FIGURE 7. Thermal susceptibility of VTAOM and BBTM 11B.

lower susceptibility to failure at low temperatures than the mixture of reference. Moreover, since variations in VTAOM behavior are with decreases in temperature, it appears that its thermal susceptibility is lower than in the case of the BBTM 11B.

Regarding resistance to aging, Figure 8 shows that VTAOM has a lower susceptibility to aging (in terms of aggregate loss) than the BBTM 11B mixture. This implies that the loss of material during its application in pavements for roads is expected to be low since this mixture showed lower sensitivity to the oxidative effect of the bitumen during its service life under climate actions such as solar radiation. Finally, both the present results and those of previous studies suggest that the UCL method is an appropriate technique for comparing the performance of

various asphalt mixes whilst permitting the analysis of the critical properties of binders (31).

### 3.2. Resistance to plastic deformations

Table 3 lists the results obtained in the cyclic triaxial test for specimens of VTAOM and BBTM 11B at 40°C. These results indicate that the VTAOM has higher accumulated deformations after a total number of 10.000 loading cycles as well as a higher creep slope during the test (which defines the sensitivity of the material to the accumulation of plastic deformations as a result of the repeated loads) and less creep modulus. Therefore, it appears that the VTAOM has lower resistance to plastic deformations than the BBTM 11B under the higher temperatures

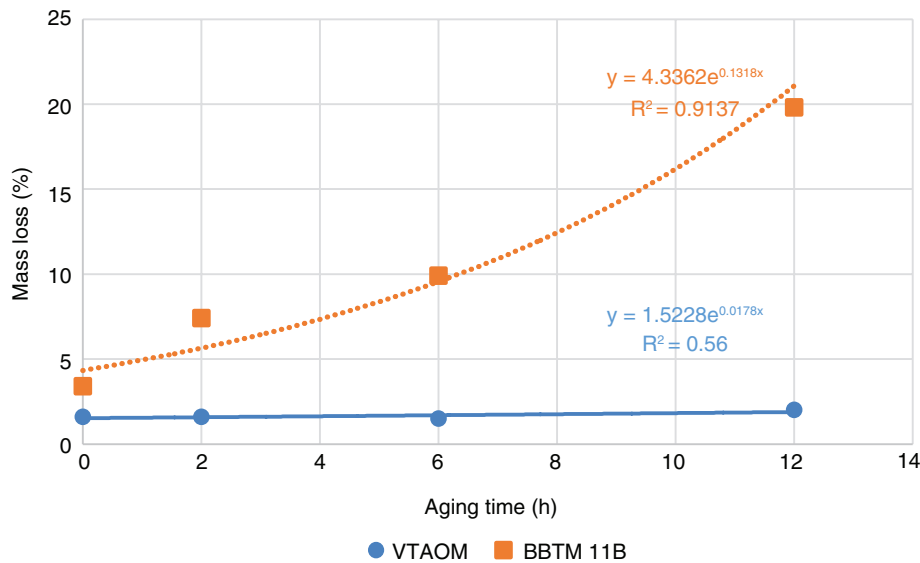


FIGURE 8. Aging resistance of VTAOM and BBTM 11B.

TABLE 3. Results of cyclic triaxial confined test.

Sample	VTAOM			BBTM 11B		
	Permanent deformation (%)	Creep slope	Modulus (kPa)	Permanent deformation (%)	Creep slope	Modulus (kPa)
1	2.16	0.36	138.89	1.38	0.27	217.39
2	2.66	0.52	112.78	1.34	0.21	223.88
3	2.30	0.79	130.43	1.40	0.32	214.29
Average	2.37	0.56	127.37	1.37	0.27	218.52
Standard deviation	0.26	0.22	13.32	0.03	0.06	4.90
Coefficient of variation (%)	10.87	39.04	10.46	2.22	20.65	2.24

that it is likely to experience during its service life. Presumably, the higher binder content could affect the resistance of VTAOM to plastic deformations. However, since VTAOM is applied with a very low thickness in urban asphalt pavements, the possible risk associated with the development of rutting is reduced while the depth of the probable rut that may occur is very limited (32). Nonetheless, other types of distresses related to plastic deformations in the tangential direction (such as shoving or corrugation) could still appear.

### 3.3. Cracking resistance and interlayer adhesiveness

The summarized results of the UGR-FACT test with applied stresses of 335 kPa and 500 kPa at different temperatures (10, 20 and 30°C) are presented in Tables 4 and 5. According to these results, BBTM 11B recorded a slightly greater bearing capacity than VTAOM (particularly under a medium stress level), which could be related to the higher thickness of the layer with the BBTM 11B mixture (35 mm) in comparison with the VTAO (20 mm),

so that the deflections appearing in the bottom of the base layer are slightly lower (Phase 1). Similarly, the increase of the bearing capacity allows for a greater protection of the base layer and thus contributes to the reduction in the speed of initiation and propagation of damage throughout the specimen (phases 2 and 3).

Nonetheless, it is important to note that the difference in behavior during these last stages is reduced (and, in fact, the VTAOM presents a higher number of cycles, and thus, higher resistance), which could be associated with higher flexibility of the VTAOM due to its higher bitumen content. In addition, according to the results displayed in Tables 4 and 5, during phase 4 both mixtures behave similarly, thus suggesting that they have similar resistance to the propagation of defects from the underlying layer (in spite of the VTAOM having a reduced thickness).

Regarding the effects of temperature, the results show that at higher temperatures there is a lower resistance to the propagation of damage in the mixtures. Thus, at high temperatures there is a

faster development of damage than at lower temperatures, where the materials have a better elastic response. In this regard, the VTAOM recorded quite similar susceptibility to temperature in terms of cracking to that measured for the mixture of reference, which indicates its suitability for application in pavements for roads. Further, the results displayed in Tables 4 and 5, suggest that both mixtures showed quite similar sensitivity to the increase in stress level.

Figure 9 shows the results of the mean damage parameter. It is clear that this parameter significantly increases when the stress level and temperature increase, which indicates higher level of damage in the asphalt layer, thereby leading to faster degradation of the bituminous material. Nonetheless, it is striking that in spite of offering a similar number of failure cycles to the BBTM 11B, the VTAOM has a lower amount of internal damage, which could be due to its stronger internal cohesion.

TABLE 4. Results of UGR-FACT test with applied stress of 335 kPa at 10, 20 and 30°C for the specimen where VTAOM and BBTM11B have been used as wearing course.

		VTAOM		BBTM11B		
Phase 4		Retention of crack				
Temperature (° C)	10	20	30	10	20	30
Average (No. cycles)	-	1,487	230	-	1,603	260
Standard deviation	-	249	121	-	770	125
Phase 3		Crack propagation in base course				
Temperature (° C)	10	20	30	10	20	30
Average (No. cycles)	-	4,357	830	-	10,137	960
Standard deviation	-	2,165	226	-	2,807	362
Phase 2		Development of damages in base course				
Temperature (° C)	10	20	30	10	20	30
Average (No. cycles)	-	23,767	1,067	-	22,767	1,333
Standard deviation	-	7,974	252	-	6,127	551
Phase 1		Deflection in the bottom of the base course				
Temperature (° C)	10	20	30	10	20	30
Average (mm)	0.0494	0.0641	0.0772	0.0482	0.0523	0.0711
Standard deviation	0.0074	0.0111	0.0057	0.0087	0.0121	0.0025

TABLE 5. Results of UGR-FACT test with applied stress of 500 kPa at 10, 20 and 30°C for the sample where VTAOM BBTM 11B have been used as wearing course.

		VTAOM		BBTM11B		
Phase 4		Retention of crack				
Temperature (° C)	10	20	30	10	20	30
Average (No. cycles)	3,800	730	65	3,500	600	40
Standard deviation	1,558	241	15	2,030	156	14
Phase 3		Crack propagation in base course				
Temperature (° C)	10	20	30	10	20	30
Average (No. cycles)	38,400	1,670	215	52,700	1,000	180
Standard deviation	14,208	685	105	47,376	340	92
Phase 2		Development of damages in base course				
Temperature (° C)	10	20	30	10	20	30
Average (No. cycles)	241,300	5,300	230	264,250	2,800	150
Standard deviation	101,346	1,961	113	77,711	1,260	59
Phase 1		Deflection in the bottom of the base course				
Temperature (° C)	10	20	30	10	20	30
Average (mm)	0.0836	0.0989	0.1631	0.0803	0.0849	0.1683
Standard deviation	0.0004	0.0049	0.0008	0.0033	0.0059	0.0134

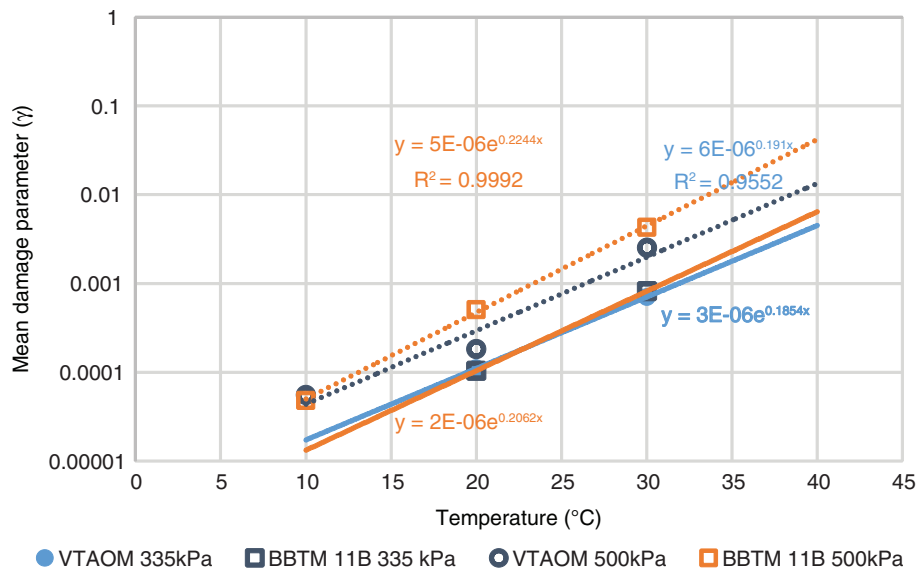


FIGURE 9. Mean damage parameter results obtained at different stress levels and temperatures.

TABLE 6. Results obtained in permeability test.

Sample	VTAOM		BBTM 11B	
	Water evacuation time (s)	Permeability coefficient (cm/s)×10 <sup>-2</sup>	Water evacuation time (s)	Permeability coefficient (cm/s)×10 <sup>-2</sup>
1	200.00	1.62	31.00	19.98
2	160.00	2.19	42.00	13.27
Average	180.00	1.91	36.50	16.63
Standard deviation	28.28	0.40	7.78	4.74
Coefficient of variation (%)	15.71	21.16	21.31	28.54

### 3.4. Permeability

The measured permeability values of the studied mixtures are shown in Table 6, which lists the time of water evacuation and the permeability coefficient. It is clear that the permeability of BBTM 11B is substantially higher than that offered by the VTAOM (due to the higher void content of the BBTM 11B mixture). Therefore, BBTM 11B reduces the presence of water on the road surface and, as a result, this mixture could reduce the risk of hydroplaning. The high content of bitumen in VTAOM and its continuous mineral skeleton are the main causes of this low permeability, and this property must be taken into account during its application in pavements, considering elements such as construction pumping, the slope of the road section, or the use of a more porous mineral skeleton.

### 3.5. Surface macrotexture

The surface macrotextures of the studied mixtures (measured using the volumetric technique) are illustrated in Table 7 as a function of the circle

TABLE 7. Measured surface macrotexture of studied mixtures.

Sample	VTAOM		BBTM 11B	
	Radio (mm)	Macrotexture depth (mm)	Radio (mm)	Macrotexture depth (mm)
1	83.00	1.20	67.00	1.80
2	84.00	1.10	61.00	2.10
Average	83.50	1.15	64.00	1.95
Standard deviation	0.71	0.07	4.24	0.21
Coefficient of variation (%)	0.85	6.15	6.63	10.88

radius and depth of the macrotexture. As can be observed, BBTM 11B provides a lower value of the radius due to greater depth of the macrotexture, so that a higher void volume is to be filled with sand. Thus the VTAOM showed lower macrotexture than the mixture of reference, providing lower friction between pavement and tire (reducing traffic safety in reference to the BBTM 11B) and thus a higher level of noise could be expected. This effect could be

associated with the continuous mineral skeleton of the VTAOM (5), which leads to a lower volume of internal and external voids.

### 3.6. Skid and wear resistance

Table 8 shows the results obtained in the skid and wear resistance tests, this last parameter being calculated as the percentage of preserved resistance after the polishing process. According to Table 8, VTAOM and BBTM 11B exhibit quite similar skid and wear resistance since they recorded similar values before the polishing process. Nonetheless, it is worth noting that the BBTM 11B showed higher sensitivity to degradation by polishing (as already observed during the internal cohesiveness test), which could reduce its skid resistance during its service life.

### 3.7. Resistance to fuels

Table 9 lists the values of the coefficients A, B, and C measured during the fuel resistance tests carried out for both asphalt mixtures. It is clear that

both mixtures show a similar resistance to fuel attacks since the value of A is lower than 5% in each mixture, whilst value of B falls within 1 and 5%. These results imply that both types of mixtures present a moderate resistance based on the EN 12697-43 standard (28).

## 4. CONCLUSIONS

This research aimed to evaluate the mechanical performance of very thin asphalt overlay mixtures (VTAOM) as a sustainable solution for the rehabilitation of urban pavements. A comparative study has been conducted between the mechanical behavior of VTAOM and a high performance overlay mixture (BBTM 11B) commonly used in pavement rehabilitation. The study was concerned with the implementation of these mixtures in urban areas and focused on both mechanical and durability features. Based on these considerations, and the results obtained from the various tests, the following conclusions can be drawn:

TABLE 8. Results of skid and wear resistance test.

Sample	VTAOM			BBTM 11B		
	Skid resistance	Resistance after Polishing	Preserved resistance (%)	Skid resistance	Resistance after Polishing	Preserved resistance (%)
1	50	48	96	49	45	92
2	50	47	94	50	45	90
3	49	46	94	49	45	92
4	46	46	100	46	45	98
Average	48.75	46.75	95.97	48.50	45.00	92.87
Standard deviation	1.89	0.96	2.86	1.73	0.00	3.41
Coefficient of variation (%)	3.88	2.05	2.98	3.57	0.00	3.67

TABLE 9. Results of fuel resistance experiment.

VTAOM												
Specimen	Density (Mg/m <sup>3</sup> )	m <sub>1,i</sub> (g)	m <sub>2,i</sub> (g)	m <sub>3,i</sub> (g)	m <sub>4,i</sub> (g)	m <sub>5,i</sub> (g)	A <sub>i</sub>	B <sub>i</sub>	C <sub>i</sub>	A	B	C
1	2.660	1183.1	1148.9	1141.8	1139.0	1135.8	2.9	1.1	4.0			
2	2.663	1185.2	1153.4	1148.5	1145.8	1143.2	2.7	0.9	3.5	3	1	4
3	2.662	1185.0	1147.2	1139.1	1138.2	1132.9	3.2	1.2	4.4			
BBTM 11B												
Specimen	Density (Mg/m <sup>3</sup> )	m <sub>1,i</sub> (g)	m <sub>2,i</sub> (g)	m <sub>3,i</sub> (g)	m <sub>4,i</sub> (g)	m <sub>5,i</sub> (g)	A <sub>i</sub>	B <sub>i</sub>	C <sub>i</sub>	A	B	C
1	2.514	1181.6	1148.1	1144.1	1134.4	1133.2	2.8	1.3	4.1			
2	2.476	1165.5	1131.1	1119.1	1115.7	1110.4	3.0	1.8	4.7	3	2	5
3	2.504	1158.2	1124.3	1113.9	1112.1	1109.7	2.9	1.3	4.2			

Note:

m<sub>1,i</sub>: The initial dry mass of the specimen before immersing in fuel (g)

m<sub>2,i</sub>: The Dry mass specimen after immersing in fuel (g)

m<sub>3,i</sub>: The mass of the specimen after being subjected to brushing for 30 s (g)

m<sub>4,i</sub>: The mass of the specimen after being subjected to brushing for 60 s (g)

m<sub>5,i</sub>: The mass of the specimen after being subjected to brushing for 120 s (g)

- According to the results obtained in the cohesiveness, adhesiveness, thermal susceptibility and ageing tests, the VTAOM has a greater internal cohesion compared with BBTM 11B, which can protect the wearing courses from possible common aggregate detachment. Similarly, VTAOM has a lower susceptibility to moisture, temperature, and aging by oxidation compared with BBTM 11B.
- The VTAOM shows greater susceptibility to plastic deformations compared with BBTM 11B. The lower resistance of the VTAOM to plastic deformation could be due to its higher bitumen content. In fact, this factor causes a lower creep modulus in the material and generates higher plastic deformations under cyclic loading. However, since the VTAOM paves very thinly (2 cm), the risk of rutting appears to be limited (although other type of distresses related to plastic deformation could appear in the tangential direction such as shoving or corrugation).
- According to the results obtained in the UGR-FACT experiments, VTAOM as a wearing course provides slightly less protection to the lower layers compared with BBTM 11B, which could be related to the decrease in the thickness of the layer. However, regarding damage propagation from the base course to the wearing course, both mixtures exhibited similar behavior although VTAOM is paved with a lower thickness.
- Concerning the experiments related to traffic safety issues and road user convenience, VTAOM is not as permeable as BBTM 11B (which could increase the risk of certain phenomena such as hydroplaning).
- Moreover, the lower macrotexture depth of VTAOM compared with BBTM 11B could prevent adequate friction with the tires and also increase noise levels, which is a matter of concern in urban areas.
- VTAOM has been proven to present appropriate skid resistance in reference to the BBTM 11B, and also recorded higher resistance in the degradation of aggregates in the wearing course layer.
- Regarding fuel resistance, VTAOM and BBTM 11B exhibited very similar behavior and they comply with the minimum requirements for these types of materials based on the standard. Thus, in urban areas — which are potentially at greater risk of fuel attacks — both mixtures appear to be acceptable alternatives for application in pavements for roads.
- Based on these results it can be concluded that the use of VTAOM could be very useful in the rehabilitation of urban pavements, as it provides both good internal cohesion (even under

different climatological, fuel, and ageing effects) and good resistance to the propagation of defects from the underlying layers. Nonetheless, it is important to note that the mineral skeleton and bitumen content of these mixtures could be improved in order to avoid the appearance of distresses related to plastic deformations (such as shoving or corrugation), as well as improving the comfort of the users by increasing its permeability and macrotexture (reducing the rolling noise and increasing the adherence between tire and pavement).

## REFERENCES

1. Alonso, A.; Tejada, E.; Moreno, F.; Rubio, M.C.; Medel, E. (2013). A comparative study of natural zeolite and synthetic zeolite as an additive in warm asphalt mixes. *Mater. Construcc* 63 [310], 195-217. <http://dx.doi.org/10.3989/mc.2013.05911>.
2. González-Taboada, I.; González-Fontebo, B.; Martínez-Abella, F.; Carro-López, D. (2016). Study of recycled concrete aggregate quality and its relationship with recycled concrete compressive strength using database analysis. *Mater. Construcc*, 66 [323], e089. <http://dx.doi.org/10.3989/mc.2016.06415>.
3. De La Garza, J.M.; Akyildiz, S.; Bish, D.R.; Krueger D.A. (2011) Network-level optimization of pavement maintenance renewal strategies. *Adv. Eng. Informatics*. 25 [4], 699–712. <http://dx.doi.org/10.1016/j.aei.2011.08.002>.
4. Chen, D.H.; Scullion, T. (2015) Very Thin Overlays in Texas. *Constr. Build. Mater.* 95, 108–16. <http://dx.doi.org/10.1016/j.conbuildmat.2015.07.157>.
5. Sandberg, U.; Kragh, J.; Goubert, L.; Bendtsen, H.; Bergiers, A.; Biligiri, K.P.; Karlsson, R.; Nielsen, E.; Olesen, E.; Vansteenkiste, S. (2011) Optimization of thin asphalt layers: state-of-the-art review. ERA-NET Road Project, European Commission – FP7, 7th Framework Programme, Deliverable No. 1.
6. Watson, D.E.; Heitzman, M. (2014) Thin asphalt concrete overlays: a synthesis of highway practice, National Cooperative Highway Research Program (NCHRP) SYNTHESIS 464, WASHINGTON, D.C., USA. (access November 21, 2016 <[http://onlinepubs.trb.org/onlinepubs/nchrp/nchrp\\_syn\\_464.pdf](http://onlinepubs.trb.org/onlinepubs/nchrp/nchrp_syn_464.pdf)>).
7. Newcomb, D.E. Thin asphalt overlays for pavement preservation, in: National Asphalt Pavement Association IS 135, National Asphalt Pavement Association, Lanham, Md., 2009 (access November 21, 2016 <<http://hawaii-asphalt.org/wp/wp-content/uploads/IS-135-Thin-Asphalt-Overlays-for-Pavement-Preservation.pdf>>).
8. Arellano, M.; Scullion, T.; Blackmore, T. (2015) Guidelines on the use of thin surface mixes for pavement preservation. In: Proceedings of Transportation Research Board 94th Annual Meeting, Washington DC, USA.
9. Hajj, E.Y.; Sebaaly, P.E.; Habbouche, J. (2016) Laboratory evaluation of thin asphalt concrete overlays for pavement preservation. Report No. SOLARIS-201601, Department of Civil and Environmental Engineering, University of Nevada, Reno, USA.
10. Mogawer, W.S.; Austerman, A.J.; Underwood, S. (2016) Effect of Binder Modification on the Performance of an Ultra-Thin Overlay Pavement Preservation Strategy. *Transp. Res. Rec. J. Transp. Res. Board* 2550, 1–7. <http://dx.doi.org/10.3141/2550-01>.
11. Read, J.; Whiteoak, D. (2003) The Shell Bitumen Handbook, fifth ed., Thomas Telford, London, (2003).
12. EN 13108-2. (2007) Bituminous mixtures, Material Specifications – Part 2: Asphalt Concrete for Very Thin Layers, AENOR, Asociación Española de Normalización y Certificación, Madrid, Spain.

13. EN 13108-1. (2008) Bituminous mixtures, Material Specifications – Part 1: Asphalt Concrete, AENOR, Asociación Española de Normalización y Certificación, Madrid, Spain.
14. Pérez Jiménez, F.; Miró Recasens, R. (1994) New methodology for asphalt binder characterisation: the UCL method. *Revista Técnica de la Asociación Española de la Carretera* 73, 27–48.
15. EN 12697-17. (2007) Bituminous mixtures. Test methods for hot mix asphalt. Part 17: Particle loss of porous asphalt specimen. AENOR, Asociación Española de Normalización y Certificación, Madrid, Spain.
16. Miró, R.; Pérez-Jiménez, F. (2001) Procedure for the evaluation of asphalt binders ageing in contact with aggregates and application of this procedure to analyze the influence of the aggregate type on binder ageing. *Road. Mater. Pavement. Des* 2 [1], 97–110. <http://dx.doi.org/10.1080/14680629.2001.9689895>.
17. EN 12697-25. (2006) Method B: Bituminous mixtures. Test methods for hot mix asphalt – Part 25: Cyclic compression test. AENOR, Asociación Española de Normalización y Certificación, Madrid, Spain.
18. Moreno-Navarro, F.; Rubio-Gómez M.C. (2013) UGR-FACT test for the study of fatigue cracking in bituminous mixes. *Constr. Build. Mater* 43, 184–90. <http://dx.doi.org/10.1016/j.conbuildmat.2013.02.024>.
19. Moreno, F.; Rubio, M.C. (2013) Effect of aggregate nature on the fatigue-cracking behavior of asphalt mixes. *Mater. Des* 47, 61–7. <http://dx.doi.org/10.1016/j.matdes.2012.12.048>.
20. Moreno-Navarro, F.; Sol-Sánchez, M.; Rubio-Gómez, M.C. (2014) Reuse of deconstructed tires as anti-reflective cracking mat systems in asphalt pavements. *Constr. Build. Mater* 53, 182–9. <http://dx.doi.org/10.1016/j.conbuildmat.2013.11.101>.
21. Moreno-Navarro, F.; Sol-Sánchez, M.; Rubio-Gómez, M.C. (2015) Exploring the recovery of fatigue damage in bituminous mixtures: the role of healing. *Road. Mater. Pavement. Des* 16, 75–89. <http://dx.doi.org/10.1080/14680629.2015.1029706>.
22. Moreno-Navarro, F.; Rubio-Gómez, M.C. (2014) Mean damage parameter for the characterization of fatigue cracking behavior in bituminous mixes. *Mater. Des* 54, 748–754. <http://dx.doi.org/10.1016/j.matdes.2013.09.004>.
23. CEDEX. (2000). Permeabilidad in situ de pavimentos drenantes con el permeámetro LCS, NLT-327/00, Dirección General de Carreteras, Madrid, Spain.
24. Fernández-Barrera, A.H.; Castro-Fresno, D.; Rodríguez-Hernández, J.; Calzada-Pérez, M.A. (2008) Infiltration Capacity Assessment of Urban Pavements Using the LCS Permeameter and the CP Infiltrometer. *J. Irrig. Drain. Eng* 134, 659-665. [http://dx.doi.org/10.1061/\(ASCE\)0733-9437\(2008\)134:5\(659\)](http://dx.doi.org/10.1061/(ASCE)0733-9437(2008)134:5(659)).
25. Georgiou, P.; Loizos, A. (2014) A laboratory compaction approach to characterize asphalt pavement surface friction performance. *Wear* 311, 114–22. <http://dx.doi.org/10.1016/j.wear.2013.12.028>.
26. CEDEX. (2000). Medida de la macrotextura superficial de un pavimento por la técnica volumétrica, NLT- 335/00, Dirección General de Carreteras, Madrid, Spain.
27. EN 1097-8. (2009) Tests for mechanical and physical properties of aggregates. Determination of the polished stone value. AENOR, Asociación Española de Normalización y Certificación, Madrid, Spain.
28. EN 12697-43. (2006) Bituminous mixtures - Test methods for hot mix asphalt - Part 43: Resistance to fuel. AENOR, Asociación Española de Normalización y Certificación, Madrid, Spain.
29. Wood, T.J.; Cole, M.K. (2013). Stripping of hot-mix asphalt pavements under chip seals. Report No. MN/RC 2013-08, Minnesota Department of Transportation, Research Services, St. Paul, Minnesota, USA.
30. Moreno-Navarro, F.; Sol-Sánchez, M.; Jiménez del Barco, A.; Rubio-Gómez, M. C. (2015) Analysis of the influence of binder properties on the mechanical response of bituminous mixtures. *Int. J. Pavement. Eng.* 1-10. <http://dx.doi.org/10.1080/10298436.2015.1057138>.
31. Jiménez del Barco-Carrión, A.; García-Travé, G.; Moreno-Navarro, F.; Martínez-Montes, G.; & Rubio-Gómez, M.C. (2016). Comparison of the effect of recycled crumb rubber and polymer concentration on the performance of binders for asphalt mixtures. *Mater. Construcc*, 66 [323], 1-9. <http://dx.doi.org/10.3989/mc.2016.08815>.
32. Barker, W.R.; Bianchini, A.; Brown, E.R.; & Gonzales, C.R. (2011) Minimum thickness requirements for asphalt surface course and base layer in airfield pavements. Final report No. ERDC/GSL-TR-11-27, Geotechnical and Structures Laboratory, U.S. Army Engineer Research and Development Center, Washington DC, USA.